An overview of high resolution infrared measurement and analysis for atmospheric monitoring of halocarbons.

Don McNaughton[1], Evan G. Robertson[2], Christopher D Thompson[1], Tarekegn Chimdi[1], Michael K. Bane[1] and Dominique Appadoo[3].*

1. School of Chemistry, Monash University, Wellington Rd., Clayton, Victoria 3800, Australia
2. La Trobe University, Department of Chemistry, Bundoora, Victoria 3086, Australia
3. Australian Synchrotron, Blackburn Rd, Clayton, Victoria 3168, Australia.

* Author to whom correspondence should be sent.
Telephone: +61-3-9905-4552
Facsimile: +61-3-9905-4597
Email: Don.McNaughton@sci.monash.edu.au

ABSTRACT

The current state of the art in recording and analyzing rotationally resolved vibration-rotation bands of atmospheric pollutant halocarbon species is reviewed. It is shown that in order to obtain molecular constants of sufficient accuracy to simulate the vibration-rotation structure over the range of atmospheric temperatures it is necessary to: Obtain spectra at a range of temperatures using static cooling cells, supersonic jet expansions and collisional cooling devices; Employ sophisticated pattern recognition and analysis software; Assign and fit spectral perturbations; Use spectral simulation and digital spectral subtraction (SASSI) to further simplify spectral bands for analysis. To demonstrate the techniques an analysis of the ν_5 band of $CH^{37}ClF_2$ in natural abundance is presented.

Keywords: vibration-rotation analysis, hydrofluorocarbons, fluorocarbons, halocarbons, high resolution FTIR.

INTRODUCTION

Infrared (IR) spectroscopy is an ideal technique for characterizing, monitoring and quantifying atmospheric molecules, be it for baseline determination of small atmospheric species or for exotic atmospheric pollutants. It thus has a significant role in environmental monitoring and is used in a variety of roles including in ground, airborne and satellite based systems. For tropospheric measurements the majority of work is carried out using medium resolution instruments because pressure and collisional line broadening limits direct atmospheric observations to resolutions > $0.1cm^{-1}$. For such work quantification relies on using model spectra simulated from well determined molecular constants or on spectral libraries. Spectral libraries are usually generated using Fourier Transform IR (FTIR) techniques and unless carefully and systematically compiled are not easily transferable to different instruments or for different applications and few useful libraries are available. Sharpe and coworkers at the Pacific Northwestern National Laboratory (PNNL) have been building a comprehensive library of spectra specifically for general use in tropospheric monitoring to fill this gap.[1] For upper atmosphere monitoring, where the spectral linewidths are much reduced, medium and high resolution techniques are required and the determinations are usually carried out using spectra "synthesized" from carefully compiled databases of line positions calculated from accurate molecular constants, together with transition cross sections and appropriate line shape parameters. A clear advantage of this approach is its ready application to samples at any temperature, pressure, or continuously varying set of these that may occur within a column profile. The **hi**gh-resolution **tran**smission molecular absorption database (HITRAN), under constant compilation at the Air Force Cambridge

Research Laboratories (AFCRL) is the best known and most widely used such database and its progress has been outlined recently by Rothman *et al* [2]. The database provides the basis for many applications in terrestrial and atmospheric remote sensing, open path monitoring, laboratory based studies and process monitoring.

The many spectrometer based satellite systems now in operation require new and more accurate data for an increasing number of molecules that require monitoring and this information comes from fundamental laboratory based experiments optimized to provide data of sufficient accuracy. One extremely important group of molecules where the essential molecular parameters are required are the ozone depleting halocarbon molecules and their replacements such as hydrofluorocarbons, most of which have significant global warming potential. Such large molecules often with numerous isotopomers, heavily populated low vibrational states and complications arising from interacting energy states have extremely rich high resolution infrared spectra. Measurement, assignment and fitting these spectra presents a challenge to even the most hardened molecular spectroscopist. In order to provide sufficient accuracy for line position and intensity prediction (and even accurate band shapes for low resolution work) over the complete range of atmospheric temperatures it is necessary to assign and fit the full range of isotopomers and their hot bands together with all perturbing states, including often "dark" states where there are no observed transitions. Recent analysis of satellite measurements of halocarbons and hydrohalocarbons[3] by the Atmospheric Trace Molecular Spectroscopy Experiment (ATMOS) and the Interferometric Monitor for Greenhouse gases (IMG) led to the conclusion that "The reliability of the existing

spectroscopic parameters has been examined, and it was found that only laboratory parameters measured at high resolution reproduce the satellite observations well".

This paper reviews the high resolution studies carried out to date for halocarbon and hydrohalocarbons and the techniques necessary to provide accurate data for the prediction of their line positions. A new analysis of the ν_5 band of chlorodifluoromethane (HCFC-22) utilizing some of these techniques is also presented.

EXPERIMENTAL

R22 ($CHClF_2$), (99% commercial grade, BOC gases Australia) was transferred to an evacuated glass multi-pass cell, set to a path length of 4m. High resolution spectra over the range 150-600 cm^{-1} were recorded with an un-apodized resolution of 0.00096 cm^{-1} on a Bruker IFS 125HR at the Australian Synchrotron using the infrared synchrotron edge radiation continuum source. The FT-IR spectrometer was equipped with a multilayer Mylar beam splitter and a liquid helium-cooled external Si:B bolometer. Over 200 scans were co-added at a sample pressure of 500 mTorr and post zero-filled with a factor of 8. Calibration was carried out by 67 H_2O and CO_2 lines in the spectra from residual traces in the interferometer compartment, using measured line positions from the HITRAN database[2] in the spectral region of 420-680 cm^{-1}.

REVIEW OF HIGH RESOLUTION STUDIES

Apart from methyl fluoride, a low molecular weight symmetric top molecule with a relatively simple structure that was thoroughly studied at high resolution in the early days of infrared spectroscopy, most fluorocarbon species required the development of

modern FTIR and laser based spectrometer systems to provide assignable high resolution data. Most work has been carried out since the advent of these systems in the 1980's with the majority of studies taking place after the realization of the ozone depleting potential of the halon containing species and the high Greenhouse warming potential of many of the fluorocarbons. Table 1 below lists the majority of the fluorocarbon-related molecules with some or all bands now characterized at high resolution to produce reliable molecular constants together with references to the work. The chloro and bromo substituted fluoroethylenes, although not considered to have major roles in atmospheric chemistry, have also been extensively studied by the groups of Gambi and Stoppa with a recent paper[78] on a band of *cis*-chlorofluoroethylene pointing to progress with these species.

REVIEW OF EXPERIMENTAL TECHNIQUES

The majority of laboratory based spectroscopy of the halocarbon and hydrohalocarbon species has been carried out using broad band FTIR spectrometers at spectral resolutions between 0.00096 and 0.005 cm^{-1} depending on the spectral region, instrument capabilities and experimental line widths, with fewer studies using either tuneable diode laser absorption spectroscopy (TDLAS) at similar resolutions to FTIR or CO_2 side band laser systems with restricted wavenumber coverage but extremely high resolution[79]. For all but the smallest molecular species the spectra at room temperature are highly congested with many thousands of individual vibration-rotation lines from the set of isotopomers and heavily populated low vibrational states. BCF, Bromochlorodifluoromethane, $CBrClF_2$ for example has 4 main isotopomers and low wavenumber modes for each of these. For example the $^{79}Br\,^{35}Cl$ isotopomer has modes at 214.5, 307, 337.7, 408.4 and 443.3 cm^{-1}.[43]

The room temperature spectrum in the upper trace of fig 1 has absorption bands that are wide due to population of states with high rotational quantum numbers and congested due to overlapping features from hot bands. Stoppa has simplified such spectra by synthesizing pure ^{81}Br and ^{79}Br isotopomers for CH_2BrF (see references in table 1) thus removing one source of overlap in room temperature spectra. In order to reduce the congestion resulting from vibrational hot bands and the highly populated rotational levels, it is necessary to cool the sample as much as possible. Some of the early TDLAS was done by simply cooling an absorption cell[18]. The restriction of course is that the lowest possible temperature is near the freezing point of the gas under study and so simple cooling is often of limited use. By far the most popular methodology is to cool the sample via supersonic expansion in the manner first used by Smalley[80] and so achieve temperatures as low as a few degrees Kelvin for small molecules, depending on the carrier gas, backing pressure, expansion nozzle diameter and pumping capacity. Herman *et al* reviewed the whole field of high resolution FTIR spectroscopy of jet-cooled molecules in 2000[81] and some of the early studies on halocarbons and hydrohalocarbons and the instrumentation developed for the work is described in that review. Most FTIR based work has been carried out by Quack's group, expanding the gases through a pinhole nozzle into a diffusion pumped vacuum chamber to intersect a single pass of the IR beam from a Bomem004 FTIR system;[82] and by McNaughton's group, using a pinhole nozzle and cryopumped vacuum system containing an 11-pass optical arrangement connected to a Bruker HR120 system[46]. These systems typically achieve rotational temperatures of 20-50 K depending on the size of the molecule under study, with vibrational degrees of freedom also cooled but to a lesser extent. The lower spectrum in

figure 1 is of jet cooled $CBrClF_2$[42], where a temperature of *ca* 40 K is achieved with significant reduction of structure in the wings of the transitions and no significant hot bands apparent in the spectrum. The group of Stoppa have recently coupled a pulsed slit jet expansion system to their diode laser systems and achieved temperatures of around 50 K for CF_3Br[26,27] and CF_3Cl[19]. With the recent developments in tunable quantum cascade lasers (QCL) for high resolution spectroscopy, reviewed by Curl[83], their usage is growing. Kelly *et al* [24] have coupled a supersonic free jet system to a QCL in a recent study on CF_3Cl.

Although jet cooling provides exceedingly simplified spectra amenable to analysis the restricted rotational quantum number range of observed transitions results in molecular constants that cannot necessarily simulate the spectrum at the higher temperatures of the atmosphere and the normal laboratory. A case in point is the ν_1 band of $C^{35}Cl_2F_2$. Giorgianni *et al* [45] used a diode laser to record a spectrum of a natural abundance sample cooled to 200 K in order to simplify the structure and assigned a set of transitions that were strong at this temperature. In order to obtain a fit they removed transitions that appeared heavily perturbed by Coriolis resonances. The subsequent fit provided a set of rotational constants that could correctly simulate only part of the spectrum at 200 K. We carried out a jet cooled study at 40 K[46] and assigned a set of low J transitions containing none of those measured by Giorgianni *et al* but less affected by resonances. This data could only simulate the spectrum correctly at very low temperatures. Figure 2, showing some data for this band from an analysis that is in progress, illustrates the problem caused by the Coriolis perturbations. The first part of the range (up to J = 20) covers the transitions assigned from the jet-cooled spectrum. The

second part (J = 25-45) corresponds to those transitions from the diode laser spectrum included in the first analysis. The final set of transitions (J > 45) were excluded from both reported fits and hence neither study could achieve the desired outcome. The use of molecular constants from incomplete analyses such as these would result in inaccurate simulations at typical atmospheric temperatures, and thereby compromise the ability to determine atmospheric concentrations.

Such problems require greater control over the range of experimental temperatures than that provided by static cooling cells or jet expansions and such a cell has been developed by Bauerecker *et al* [84] and coupled to a TDLAS system and FTIR spectrometer. Bauerecker's multipass cell allows for enclosive flow cooling or collisional cooling at temperatures between 4-400 K and in enclosive flow mode allows for cooling below the normal freezing point of samples. We built a simple dual pass system of similar design and used it to simplify the spectra of a range of halocarbons.[38-40,56,58,64-66] Figure 3 shows one such example, CF_3CH_2F, and illustrates the benefits of being able to analyse spectra measured at a range of different temperatures to maximise the set of assignable transitions. More recently we have, in collaboration with Bauerecker, built a full multipass system and have coupled it to the high resolution Bruker HR125 spectrometer on the infrared beamline of the Australian synchrotron. The group of Quack have also coupled a Bauerecker cell to a high resolution FTIR instrument and have used it recently to obtain spectra of $CHCl_2F$.[50]

REVIEW OF ANALYSIS TECHNIQUES

For molecules such as the fluorocarbons where successful simulation of the spectrum from molecular constants is desired it is essential to assign and fit all the features in a

spectrum, recognizing and treating all perurbations. The many thousands of individual rotational lines in a single vibrational band present a challenge in initial assignment and this is achieved by utilizing computer assisted methods based primarily on Loomis-Wood plots[85]. In its original graphical interface mode on either a PC[86] or Mac[87] the Loomis-Wood technique treated the spectrum as that of a linear molecule where the line spacings of the P and R branches are approximately 2 times the rotational constant *B* and the line positions can be fitted by a polynomial expansion of a running variable that is related to the rotational angular quantum number *J*, where the coefficients are related to the molecular constants. The technique uses a peaklist, containing position and intensity information, generated from the spectrum and re-plots the spectrum in rows of adjacent sections one under another where the successive section widths are a function of the polynomial coefficients. For a hypothetical linear molecule with the *B* rotational constant the same in upper and lower energy states and no centrifugal distortion each section would be 2*B* wide and the related transitions would appear as a perfect vertical line on the plot. Peaks can then be selected, ground state combination differences automatically calculated to check assignments and the assigned lines fitted with an appropriate Hamiltonian. Any perturbations in the spectrum (such as those in figure 2) are readily recognized in the Loomis plots and the technique is readily adapted to symmetric tops. Even asymmetric tops have branches of lines with almost equivalent line spacings that slowly change with quantum number so the original programs are also useful for the assignment of asymmetric top molecules, as shown in figure 4a where a MacLoomis plot of the *P* branch of the ν_2 band of $CHClF_2$.in natural abundance is shown. Intense K_a subbands are easily observed. Recently, new versions[88-90] have appeared with extended

capabilities that are designed to allow the assignment of almost any molecule and provide direct input into fitting and simulation programs such as Pickett's SPFIT and SPCAT[91]. The Loomis plot allows the assignment of regularly spaced series of transitions based on visual pattern recognition through a graphical interface and is extremely useful for assigning well resolved and/or prominent spectral transitions. However, by reducing the spectrum to a list of peaks some information is invariably lost, e.g. when shoulder or coincident peaks are not detected as separate features and numerous weak peaks from hot bands or low abundance isotopomers become essentially a noisy background in the graphical plot. When a weak band is obscured or overlapped by a stronger one the reduction in distinct peaks associated with the weaker band in the graphical plot may also prevent recognition of the pattern of its regularly spaced lines, and reduce the possibility of successful rovibrational assignments. The information extracted from high resolution IR spectra may be enhanced by digitally subtracting contributions from one or more components, obtained through simulation of their rovibrational structure, an approach we have named SASSI (Spectral Assignment by Simulated Spectral Intensities). With a simple molecule like ClSN,[92] SASSI allowed 7 different spectral contributions from 3 different isotopomers and 4 hot bands to be extracted and assigned. Its application to the ν_2 (1313.1 cm^{-1}) and ν_7 (1351.7 cm^{-1}) bands of $CHClF_2$ [39] led to rovibrational line assignments for less intense and overlapping features. The number of transitions assigned to the fundamental bands of the two chlorine isotopomers increased from 9217 to 15695 with a greater range of rotational quantum numbers than found in a previous study and three hotbands otherwise completely obscured in the observed spectrum were assigned. Figure 5c shows a section of the spectrum that results from subtracting a simulated

$CH^{35}ClF_2$ spectrum (fig 5b) from the original (fig 5a). Comparison of the resultant spectrum (fig 5c) with a simulated $CH^{37}ClF_2$ spectrum (fig 5d), reveals how the $CH^{37}ClF_2$ peaks that were completely obscured in the raw experimental spectrum are effectively exposed. Subsequent subtraction of the $CH^{37}ClF_2$ features allowed us to assign the remaining structure belonging to hot bands and eventually simulate successfully both full bands. The MacLoomis plot of figure 4 shows the power of the SASSI approach where in fig 4b the strong lines of ν_2 for both chlorine isotopes of $CHClF_2$ have been subtraction out prior to peak-picking and subsequent analysis. The lines that now emerge are due to hot bands that comprise some 17% of the total intensity of the band. The low K_a structure of one of the 3 hot bands assigned, $2_0^1 9_1^1$ is highlighted.

Successful simulation and indeed SASSI analysis of a whole spectral band depends also on ascertaining and fitting all Coriolis and anharmonic (e.g. Fermi) resonances. These may cause local avoided crossings such as those evident in figure 2 as well as more global perturbations. Work on the Coriolis coupled ν_3 and ν_8 band system of $CHClF_2$[40] provides an excellent example of how the full gamut of MacLoomis, collisional cooled spectra (150 K), room temperature spectra and SASSI are required to reach a successful assignment and simulation. In order to assign, fit and simulate the complete band it was necessary to include two "dark" states that perturb three different parts of the spectrum in the procedure. Dark states are those for which no transitions would normally be observable and are usually weak combination bands. After final SASSI subtraction, the interacting states and resonances shown in figure 6 were all understood and assigned. A number of lines associated with the "dark" $3\nu_9$ state that appear with sufficient borrowed intensity were correctly simulated and assigned.

ANALYSIS OF R22 ($CH^{37}ClF_2$) ν_5

Chlorodifluoromethane (also known as HCFC-22, R-22, Genetron 22 or Freon 22) is used in air conditioning applications as an alternative to the ozone depleting CFC-11 and CFC-12 molecules. R22 itself has an ozone depletion potential of 0.05 and a global warming potential (GWP) of 1780 [93] and as a consequence has been phased out in 2010. R22 is a near-prolate asymmetric top, which belongs to the C_s symmetry point group and has 6 vibrational modes with symmetry species of A'(A/C-type bands) and 3 modes of symmetry A'' (B-type bands). All nine bands have been extensively studied. Both experimental and *ab-initio* vibrational assignments for R22 are summarized in the works of Thompson *et.al*[38,39], and Gambi *et.al* [31]. For the ν_5 (A/C- type band), Gambi *et.al.*[31]and Klatt *et.al.*[36] performed high resolution FTIR and microwave spectroscopic studies respectively of the dominant isotope, $CH^{35}ClF_2$. Gambi reported that the large density of lines in the spectrum and the overlap with stronger absorptions coming from $CH^{35}ClF_2$ made the analysis of $CH^{37}ClF_2$ very difficult so that an assignment and analysis was not achieved. We have now succeeded in analysing the $CH^{37}ClF_2$ band using the SASSI approach.

The experimental spectrum of the ν_5 band of $CHClF_2$ is shown in fig. 7 and a small section of this experimental spectrum is shown in Fig 8a. The excellent sets of constants provided for ν_5 of the ^{35}Cl species by Klatt et al [36] and for the ground state by Kisiel et al[37] were used to first predict line intensities and positions of the ^{35}Cl ν_5 band using SPCAT[91] which were then convolved using a Gaussian lineshape function of appropriate full width half height to simulate the spectrum, a small part of which is

shown in fig 8b. This spectrum was then subtracted from the experimental spectrum to obtain the new spectrum shown in fig 8c where the ^{37}Cl species dominates. The optimum subtraction was achieved in an iterative fashion to determine the correct ratio of A and C type components for subtraction and to determine the Herman Wallis factors[94] that severely affected the relative intensities of the C type component. The resultant spectrum (a small section is shown in Fig 8c) was then peak picked and the data analysed using MacLoomis[87]. The ground state constants of $CH^{37}ClF_2{}^{37}$ were used to calculate ground state combination differences and confirm the assignment and the assigned lines then fitted with Pickett's SPFIT program to obtain the constants of table 2. There was no evidence of local avoided crossings or other resonance perturbations and the derived constants are well determined and comparable in magnitude and sign with those of the ^{35}Cl species. The higher order centrifugal distortion constants were held to those of the ground state in the fit. Simulation of the $CH^{37}ClF_2$ spectrum, shown in figure 8d, shows much of the spectrum in 8c is due to the $CH^{37}ClF_2$ fundamental. The remaining spectral features are due to hot bands. From the spectral simulations the dipole derivate ratio μ_a^2: μ_c^2 is 0.38:1 and the Herman Wallis factor = -0.004 for the ^{35}Cl species. No standard deviations are given because these parameters are merely those that result in the optimum spectral subtraction and given the complex overlapping spectral bands that constitute the spectrum such an exercise can only produce approximate answers. Now that both isotopic species have been assigned and simulated a complete analysis of the intensities to derive accurate Herman-Wallis should be possible leading to analysis of the more intense hot band structure.

CONCLUSIONS

The experimental and analysis techniques required to obtain molecular constants of sufficient accuracy to provide simulated spectra of use in the quantification of atmospheric pollutant species using high resolution infrared spectroscopy have been reviewed. Such constants, together with line intensity parameters also provide an accurate basis for the prediction of band profiles for low resolution atmospheric identification and quantification. The ν_5 band of chlorodifluoromethane in natural abundance has been recorded at un-apodized resolution of 0.00096 cm^{-1}, analysed using a Loomis-Wood based program and Spectral Assignment by Simulated Spectral Intensities (SASSI) and fitted to produce a set of accurate molecular constants for $CH^{37}ClF_2$.

ACKNOWLEDGEMENTS

The authors thank the Australian synchrotron for beamtime on the high resolution infrared line. MB is supported by a Monash University Faculty of Science post graduate scholarship.

1. Sharpe, S. W.; Johnson, T. J.; Sams, R. L.; Chu, P. M.; Rhoderick, G. C.; and Johnson, P. A. *Appl. Spectrosc*. **2004**, 58, 1452–1461.

2. Rothman, L. S.; Gordon, I. E.; Barbe, A.; Benner, D. Chris; Bernath, P. F.; Birk, M.; Boudon, V.; Brown, L. R.; Campargue, A.; Champion, J.-P.; Chance, K.; Coudert, L. H.,; Dana, V.; Devi, V. M.; Fally, S.; Flaud, J.-M.; Gamache, R. R.; Goldman, A.; Jacquemart, D.; Kleiner, I.; Lacome, N.; Lafferty, W. J.; Mandin, J.-Y.; Massie, S. T.; Mikhailenko, S. N.; Miller, C. E.; Moazzen-Ahmadi, N.; Naumenko, O. V.; Nikitin, A. V.; Orphal, J.; Perevalov, V. I.; Perrin, A.; Predoi-Cross, A.; Rinsland, C. P.; Rotger, M.; Šimečková, M.; Smith, M. A. H.; Sung, K.; Tashkun, S. A.; Tennyson, J.; Toth, R. A.; Vandaele, A. C.; Vander Auwera, J. *J. Quant. Spec. Rad. Transfer* **2009**, *110*, 533–572.

3. Coheur, P. F.; Clerbaux, C.; Colin, R, *J. Geophys. Res, (Atmospheres)* **2003**, *108*, 4130.

4. Smith, K. M.; Duxbury, G.; Newnham, D. A.; Ballard, J. *J. Mol. Spectrosc*. **1999**, *193*, 166-173.

5. Baldacci, A.; Stoppa, P.; Giorgianni, S.; Visinoni, R.; Ghersetti, S. *J. Mol. Spectrosc.* **1993**, *159*, 481-93.

6. Baldacci, A.; Stoppa, P.; Giorgianni, S.; Ghersetti, S. *J. Mol. Spectrosc.* **1999**, *194*, 73-78.

7. Baldacci, A.; Stoppa, P.; Giorgianni, S.; Visinoni, R.; Baldan, A. *J. Mol. Spectrosc.* **1997**, *183*, 388-397.

8. Baldacci, A.; Stoppa, P.; Giorgianni, S.; Visinoni, R. *J. Mol. Spectrosc*. **1996**, *177*, 106-114.

9. Baldacci, A.; Stoppa, P.; Giorgianni, S.; Visinoni, R.; Ghersetti, S. *J. Mol. Spectrosc.* **1994**, *166*, 264-72.

10. Stoppa, P.; Baldacci, A.; Visinoni, R.; Giorgianni, S. *Molecular Physics* **2006**, *104*, 3187-3192.

11. Baldacci, A.; Stoppa, P.; Giorgianni, S.; Wugt Larsen, R. *J. Mol. Spectrosc.* **2008**, *251*, 123-128.

12. Baldacci, A.; Stoppa, P.; Pietropolli Charmet, A.; Giorgianni, S.; Cazzoli, G.; Cludi, L.; Puzzarini, C.; Wugt Larsen, R. *J. Mol. Spectrosc*. **2007**, *246*, 126-132.

13. Baldacci, Agostino; Stoppa, Paolo; Pietropolli Charmet, Andrea; Giorgianni, Santi; Cazzoli, Gabriele; Puzzarini, Cristina; Larsen, Rene Wugt. J. Phys. Chem. A **2007**, *111*, 7090-7097.

14. Baldacci, A.; Stoppa, P.; Pietropolli Charmet, A.; Giorgianni, S. *J. Mol. Spectrosc.* **2003**, *220*, 7-12.

15. Baldacci, A.; Stoppa, P.; Gambi, A. *J. Mol. Spectrosc*. **2000**, *201*, 280-284.

16. Amrein, A.; Hollenstein, H.; Locher, P.; Quack; M. Schmitt; U. Bürger, H.; *Chem. Phys. Lett*. **1987**, *139*, 82-88.

17. Nencini, L.; Snels, M.; Hollenstein, H.; Quack, M. *Mol. Phys*. **1989**, *67*, 989-1009.

18. Baldacchini, G.; Bizzarri, A.; Nencini, L.; Snels, M.; Giorgianni, S.; Ghersetti, S. *J. Mol. Spectrosc.* **1988**, *130*, 337-43.

19. Pietropolli Charmet, A.; Stoppa, P.; Toninello, P.; Giorgianni, S.; Ghersetti, S. *Phys. Chem. Chem. Phys.* **2003**, *5*, 3595-3599.

20. Giorgianni, S.; Stoppa, P.; De Lorenzi, A.; Ghersetti, S. *J. Mol. Spectrosc*. **1992**, *154*, 265-76.

21. Giorgianni, S.; Stoppa, P.; Baldacci, A.; Gambi, A.; Ghersetti, S. *J. Mol. Spectrosc.* **1991**, *150*, 184-94.

22. Hollenstein, H.; Quack, M. *Mol. Phys*. **1989**, *68*, 759-764.

23. Stoppa, P; Gambi, *J. Mol. Struct*. **2000**, *517*, 209-216.

24. Kelly J. F.; Maki A.; Blake T. A.; Sams R. L. *J. Mol. Spectrosc*. **2008**, *252*, 81-89.

25. Bürger, H.; Burczyk, K.; Hollenstein, H.; Quack, M. *Mol. Phys*. **1985**, *55*, 255-275.

26. Pietropolli Charmet, A.; Tasinato, N.; Stoppa, P.; Baldacci, A.; Giorgianni, S. *Mol. Phys.* **2008**, *106*, 1171-1179.

27. Pietropolli Charmet, A.; Stoppa, P.; Toninello, P.; Baldacci, A.; Giorgianni, S. *Phys. Chem. Chem. Phys.* **2006**, *8*, 2491-2498.

28. (a) Visinoni, R.; Baldacci, A.; Giorgianni, S.; Stoppa, P.; Ghersetti, S. *J. Mol. Spectrosc.* **1990**, *140*, 162-9. (b) Amrein, A.; Locher, P.; Quack M.;. Schmitt, U. COMET **1987**, *10*, 9-11.

29. Amrein, A.; Hollenstein, H.; Quack,; M. Schmitt, U. *Infrared Physics* **1989**, *29*, 561-574.

30. Albert, S.; Hollenstein, H.; Quack, M.; Willeke.;M. *Mol. Phys.* **2006**, *104*, 2719 – 2735.

31. Gambi, A.; Stoppa, P.; Giorgianni, S.; De Lorenzi, A.; Visinoni, R.; Ghersetti, S. *J. Mol. Spectrosc*. **1991**, *145*, 29-40.

32. Albert, S.; Hollenstein, H.; Quack, M.; Willeke.;M. *Mol. Phys* **2004**, *102*, 1671–1686

33. Snels, M.; D'Amico, G. *J. Mol. Spectrosc.* **2001**, *209*, 1-10.

34. Luckhaus D.; Quack, M. *Mol. Phys*. **1989**, *68*, 745-758.

35. Ross, J.; Amrein, A.; Luckhaus D.; Quack, M. *Mol. Phys.* **1989**, *66*, 1273-1277.

36. Klatt, G.; Graner, G.; Klee, S.; Mellau, G.; Kisiel, Z.; Pszczolkowski, L.; Alonso, J. L.; Lopez, J. C. *J. Mol. Spectrosc.* **1996**, *178*, 108-112.

37. Kisiel, Z.; Alonso, J. L.; Blanco, S.; Cazzoli, G.; Colmont, J. M.; Cotti, G.; Graner, G.; Lopez, J. C.; Merke, I.; Pszczolkowski, L. *J. Mol. Spectrosc*. **1997**, *184*, 150-155.

38. Thompson, C. D.; Robertson, E. G.; McNaughton, *Chem. Phys.* **2002**, *279*, 239-248.

39. Thompson, C. D.; Robertson, E. G.; McNaughton, D. *Phys. Chem. Chem. Phys*. **2003**, *5*, 1996 – 2000.

40. Thompson, C. D.; Robertson, E. G.; McNaughton, D. *Mol. Phys.* **2004**, *102*, 1687-1695.

41. Bauder, A.; Beil, A.; Luckhaus, D.; Müller F.; Quack, M. *J. Chem. Phys*. **1997**, *106*, 7558-7570.

42. McNaughton D.; McGilvery, D.; Robertson, E. G. *J. Mol. Struct*. **1995**, *348*, 1-4.

43. McNaughton D.; Robertson, E. G.; Shanks, F. *Chem. Phys.* **1996**, *206*, 161-171.

44. D'Amico, G.; Snels, M.; Hollenstein, H.; Quack, M. *Phys Chem Chem Phys* **2002**, *4*, 1531-1536.

45. Giorgianni, S.; Gambi, A.; Baldacci, A.; De Lorenzi, A.; Ghersetti, S. *J. Mol. Spectrosc.* **1990**, *144*, 230-8.

46. McNaughton D.; McGilvery, D.; Robertson, E. G. *J. Chem. Soc. Faraday Trans.* **1994***, 90*, 1055 - 1071.

47. Smith, K.M.; Duxbury, G; Newnham, D.A., Ballard, J.; *J. Mol. Spectrosc.* **2002**, *212*, 6-16.

48. Amrein, A.; Quack, M.; Schmitt, U. *Mol. Phys*. **1987**, *60*, 237-248.

49. Dübal H. R.; Quack, M. *Chem. Phys. Lett*. **1981**, *80*, 439-444.

50. Albert, S.; Bauerecker, S.; Quack, M.; Steinlin.; A. *Mol. Phys.* **2007**, *105*, 541–558.

51. Albert, S.; Albert, K. K.;. Quack, M. *J. Mol. Struct*. **2004**, *695-696*, 385–394

52. Snels, M.; Beil, A.; Hollenstein, H.; Quack, M.; Schmitt, U.; D'Amato, F. *J. Chem Phys* **1995**, *103*, 8846-53.

53. Snels, M.; D'Amico, G.; Piccarreta, L.; Hollenstein, H.; Quack, M. *J. Mol. Spectrosc.* **2001**, *205*, 102-109.

54. Hollenstein, H.; Quack M.; Richard, E. *Chem. Phys. Lett*. **1994**, *222*, 176-184.

55. Baldacci, A.; Giorgianni, S.; Stoppa, P.; De Lorenzi, A.; Ghersetti, S. *J. Mol. Spectrosc.* **1991**, *147*, 208-14.

56. Chimdi T.; Robertson, E. G.; Puskar, L.; Thompson, C. D.; Tobin, M. J.; McNaughton, D. *Chem. Phys. Lett.* **2008**, *465*, 203-206.

57. Chimdi T.; Robertson, E. G.; Puskar, L.; Thompson, C. D.; Tobin, M. J.; McNaughton, D. *J. Mol. Spec* **2008,** *251*, 256-260.

58. Appadoo, D. T.; Robertson, E. G.; McNaughton, D. *J. Mol. Spectrosc.* **2003**, *217*, 96-104.

59. McNaughton D.; Robertson, E. G.; Evans, C. *Mikrochim. Acta* **1997**, *S14*, 543 - 546.

60. McNaughton D.; and Evans, C. *J. Mol. Spec*. **1997**, *182*, 342-349.

61. Duxbury, G.; McPhail, M. J. W; Smith, K. W.; Nivellini, G.; Tullini, F.; Celli, A. *J. Mol. Spectrosc.* **2000**, *199*, 13-17.

62. Duxbury, G; McPhail, M. J. W.; Smith, K. M., et al *J. Mol. Spectrosc*. **2000**, *199*, 13-17.

63. Thompson, C. D.; Robertson, E. G.; Aleksic, I.; McNaughton, D. *J. Mol. Spectrosc.* **2005**, *230*, 133-138.

64. McNaughton, D.; Aleksic, I.; Appadoo, D. T.; Thompson, C. D.; Robertson, E. G. *Vibrational Spectroscopy* **2004**, *36*, 123-128.

65. Thompson, C. D.; Robertson, E. G.; Evans, C.; McNaughton, D. *J. Mol. Spec*. **2003**, *218*, 48-52.

66. McNaughton D.; and Evans, C.; Robertson, E. G. *J. Chem. Soc. Faraday Trans* **1995**, *91,* 1723-1728.

67. Snels, M.; D'Amico, G. *J. Mol. Spectrosc.* **2003**, *221*, 156-162.

68. Xu, LH; Andrews, AM; Cavanagh, RR, et al *J Phys. Chem A* **1997**, *101*, 2288-2297.

69. Ward, K. M.; Duxbury, G.; Lorono, M.; Henze, W.; Davies, P. B.; Newnham, D. A. *J. Mol. Spectrosc.* **2000**, *204*, 268-274.

70. Robertson, E. G.; Thompson, C. D.; Appadoo, D. T.; McNaughton, D. *Phys. Chem. Chem. Phys*. **2002**, *4*, 4849 – 4854.

71. McNaughton D.; and Evans, C. *J. Phys. Chem*. **1996**,*100*, 8660-8664.

72. di Lauro, C.; D'Amico, G.; Snels, M. *J. Mol. Spectrosc.* **2009**, *254*, 108-118.

73. D'Amico, G.; Snels, M. *J. Mol. Spectrosc.* **2003**, *217*, 72-78.

74. Snels, M.; D'Amico, G. *European Physical Journal D*: **2002**, *21*, 137-142.

75. Baskakov, O. I. ; Ilyushin, V. V.; Alekseev, E. A., Bürger, H.;

Pawelke, G. *J. Mol. Spectrosc*. **2000**, *202*, 285-292.

76. McNaughton D.; and Evans, C. *Spectrochim. Acta.* **1999**, *55*, 1177-1183.

77. Hollenstein, H.; Quack, M.; Thöne, H. J. *Mol. Phys*. **1985**, *56*, 463-477.

78. Gambi, A; Stoppa, P; Tamassia, F. *J. Mol. Spectrosc.* **2008**, *252*, 47-51.

79. Stone, S. C.; Miller, C. C.; Philips, L. A.; Andrews, A. M.; Fraser, G. T.; Pate, B. H.; Xu, L.H. *J. Mol. Spectrosc*. **1995**, *174*, 297-318.

80. Smalley, R.E.; Wharton L.; Levy D. H. *Acc. Chem. Res.;* **1977**, *10*, 139–145.

81. Herman M.; Georges R.; Hepp M.; Hurtmans D. *Int. Rev Phys Chem*, **2000**, *19*, 277-325.

82. Èbal, H. R.; Quack, M.; Schmitt, U. *Chimia* , **1984**, *38*, 438.

83. Curl, R. F.; Capasso, F.; Gmachl, C.; Kosterev, A. A.; McManus, B.; Lewicki, R.; Pusharsky, M.; Wysocki, G.; Tittel, Frank K. *Chem. Phys. Lett.* **2010**, *487*, 1-18.
84. Bauerecker, S.; Taraschewski, M. ; Weitkamp, C. ; Cammenga, H. K. *Rev. Sci. Instr.* **2001**, *72*, 3946-3955.
85. Loomis, F.W.; Wood, R. W. *Phys Rev.* **1928**, *32*, 223.
86. Winnewisser, B. P.; Reinstaedtler, J.; Yamada, K. M. T.; Behrend, J. *J. Mol. Spectrosc*. **1989**, *136*, 12-16.
87. McNaughton, D.; McGilvery, D.; Shanks, F. *J. Mol. Spectrosc*. **1991,** 149, 458-73
88. Medvedev, I. R.; Winnewisser, M.; Winnewisser, B. P.; De Lucia, F. C.; Herbst, E. *J. Mol. Struct.* **2005**, *742*, 229-236
89. Lodyga, W.; Kreglewski, M.; Pracna, P.; Urban, S. *J. Mol. Spectrosc*. **2007**, *243*, 182-188.
90. Tasinato, N.; Pietropolli Charmet, A.; Stoppa, P. *J. Mol. Spectrosc*. **2007,** 243, 148-154.
91. Pickett H. M. *J. Mol. Spectrosc***. 1991**, *148*, 371–377.
92. Robertson, E. G.; McNaughton, D. *J. Mol. Spectroc.* **2006**, *238*, 56-63.
93. Intergovernmental Panel on Climate Change/Technology and Economic Assessment Panel. Special Report on Safeguarding the Ozone Layer and the Global Climate System; Issues Related to Hydrofluorocarbons and Perfluorocarbons; Cambridge University Press: Cambridge, **2006**.
94. Herman, R.; Wallis, R.F *J. Chem. Phys.* **1955**, *23* 637-646.

Figure 1. (a) Room temperature spectrum of $CBrClF_2$ at $0.01cm^{-1}$ resolution; (b) Jet-cooled spectrum of $CBrClF_2$ at an effective resolution of $0.005cm^{-1}$. The rotational temperature is *ca* 40 K.

Figure 2. Residuals (obs-calc) versus rotational quantum numbers for an effective fit without Coriolis interactions of ν_1 fundamental transitions in $C^{35}Cl_2F_2$. (From unpublished analysis in progress).

Figure 3. (a) Jet cooled spectrum of CF_3CH_2F at *ca* 65 K; (b) collisional cooled spectrum of CF_3CH_2F *ca* 150K; (c) room temperature spectrum of CF_3CH_2F. The arrows indicate Q branch heads of hot bands. (from ref. 65).

Figure 4. Macloomis plots of (a) the observed ν_2 spectrum of $CHClF_2$ with cold sub-bands of the $CH^{35}ClF_2$ species highlighted and (b) the resultant spectrum after SASSI of the cold bands of both isotopic species showing features. Lines associated with the $2_0^1 9_1^1$ and $2_0^1 6_1^1$ hotbands can mostly be seen in (b) the resultant spectrum. Figure taken from ref 39.

Figure 5 (a) Expanded high resolution FTIR spectrum of the ν_7 band of $CHClF_2$, together with (b) a simulation of the dominant $CH^{35}ClF_2$ component (c) the resultant spectrum after the $CH^{35}ClF_2$ component has been subtracted, and (d) a $CH^{37}ClF_2$ simulation. Simulations are based on experimentally derived spectroscopic parameters from reference [39].

Figure 6**.** Energy level diagram showing the Coriolis resonance interactions between vibrational states of $CH^{35}ClF_2$.

Figure 7. High resolution FTIR spectrum of the ν_5 band of $CHClF_2$.

Figure 8. (a) Expanded spectrum of the ν_5 band of $CHClF_2$, together with (b) a $CH^{35}ClF_2$ simulation, (c) the resultant spectrum after the $CH^{35}ClF_2$ component has been subtracted, and (d) a $CH^{37}ClF_2$ simulation. Simulations are based on the spectroscopic parameters in table 2, with μ_a^2: μ_c^2 of 0.38:1, the Herman Wallis factor -0.004 (coded 50013 in the Pickett program) for the ^{35}Cl species, T_{rot}=300 K and a Gaussian full width half-maximum linewidth of 0.0014 cm^{-1}.

Table 1. Fluorocarbon-related species studied by high resolution infrared spectroscopy.

Molecular formula	Name	References
CH_2F_2	HFC-32	4
CH_2ClF	HCFC-31	5-9
CH_2BrF	CFC-31B1	10-15
CF_3Cl	CFC-13	16-24
CF_3Br	Halon 1301	25-29
$CHClF_2$	HCFC-22	30-40
$CHBrF_2$	Halon 1201	*
CHBrClF	FC21B1	41
CF_2ClBr	Halon 1211	42,43
CF_2Cl_2	CFC-12	44-46
CF_2Br_2	Halon 1202	*
CHF_3	HFC-23	25,47-49
$CHCl_2F$	HFC-21	50,51
$CHBr_2F$	Halon1102	*
$CFCl_3$	CFC-11	52,53
CF_3I	Freon13T1	54,55,24
CH_3CH_2F	HFC-161	*
CH_3CHF_2	HFC 152a	56-60
CH_3CF_3	HFC 143a	61,62
CF_3CHF_2	HFC 125	63,64
CF_3CH_2F	HFC134a	65-68
C_2F_6	FC-116	69
C_2F_4	Tetrafluoroethylene	70
CH_3CF_2Cl	HCFC-142b	71-75
CF_3CHFCF_3	HFC-227ea	76
$(CH_3)_3CF$	t-butyl fluoride	77

* species with no available high resolution data to date.

Table 2. Fitted spectroscopic constants (cm^{-1}) in Watson's *A*-reduced I^r Hamiltonian for the ν_5 band of $CH^{37}ClF_2$.

constant	G.S - $CH^{37}ClF_2$[i]	ν_5 - $CH^{35}ClF_2$[ii]	ν_5 - $CH^{37}ClF_2$
band centre	-	596.371399 (5)[iii]	595.4803364 (194)
A	0.341364817	0.3404517107(70)	0.340418743 (43)
B	0.157347146	0.1621428 (11)	0.157344031 (104)
C	0.114474126	0.11698364 (31)	0.114465388 (21)
$\Delta_J\times10^6$	0.049588272	0.0523657 (23)	0.049762 (38)
$\Delta_{JK}\times10^6$	0.148145488	0.1526536 (70)	0.146941 (127)
$\Delta_K\times10^6$	0.171658755	0.161257 (11)	0.169396 (94)
$\delta_J\times10^6$	0.013769993	0.01474186 (80)	0.0138022 (192)
$\delta_K\times10^6$	0.162488411	0.166429 (17)	0.161827 (208)
$\Phi_J\times10^{12}$	0.0216642	0.02104 (47)	0.0216642[iv]
$\Phi_{JK}\times10^{12}$	0.3471063	0.376 (11)	0.3471063[iv]
$\Phi_{KJ}\times10^{12}$	-0.1035720	-0.178 (33)	-0.1035720[iv]
$\Phi_K\times10^{12}$	0.1741206	0.196 (23)	0.1741206[iv]
$\phi_J\times10^{12}$	0.0101703	0.01050 (17)	0.0101703[iv]
$\phi_{JK}\times10^{12}$	0.1870627	0.1961 (63)	0.1870627[iv]
$\phi_K\times10^{12}$	3.1481772	3.152 (56)	3.1481772[iv]
J_{max}	-	78	94
number trans.	-	7996[ii]	3804
rms deviation/cm^{-1}	-		0.000441
σ_{dev}	-		1.0996

[i] Ground state constants from Ref [37].[ii] ν_5 - $CH^{35}ClF_2$constants from Ref [36] obtained from fit to 7788 IR lines and 208 microwave lines.[iii] Figures in brackets are one standard deviation according to the least squares fit in units of the least significant figure quoted. [iv]Sextic constants have been constrained to their respective ground state values.

Fig 1.

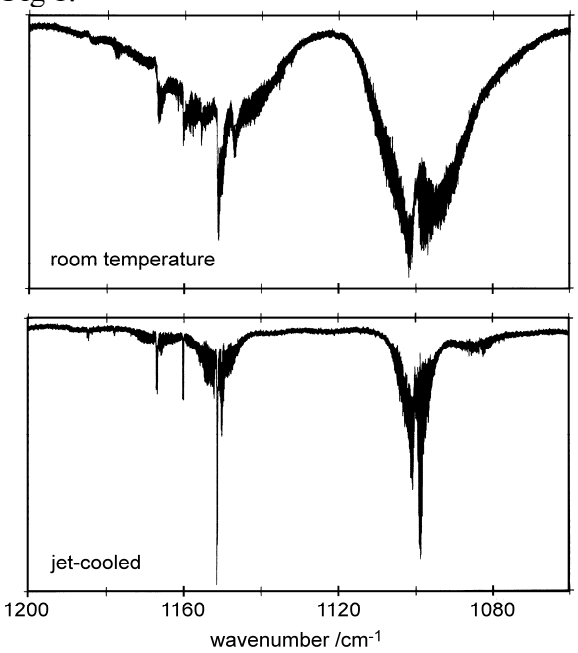
room temperature
jet-cooled
1200
1160
1120
1080
wavenumber /cm-1

Fig 2

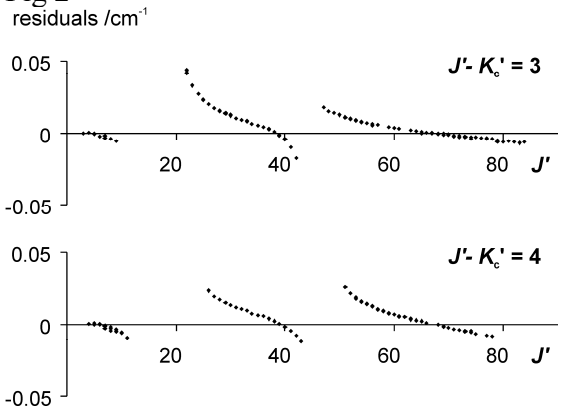
residuals /cm-1
0.05
0
-0.05
J'- Kc' = 3
20
40
60
80
J'
0.05
0
-0.05
J'- Kc' = 4
20
40
60
80
J'

Figure 3

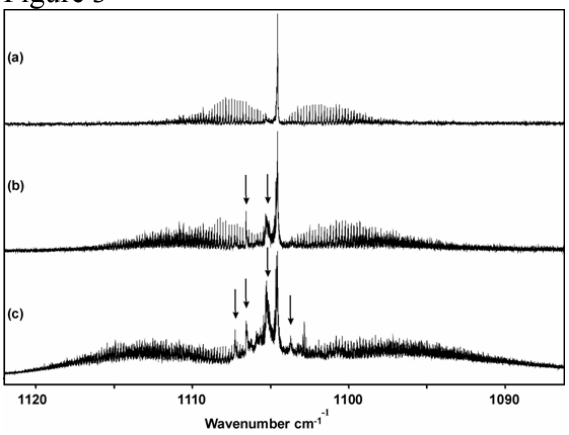

Figure 4

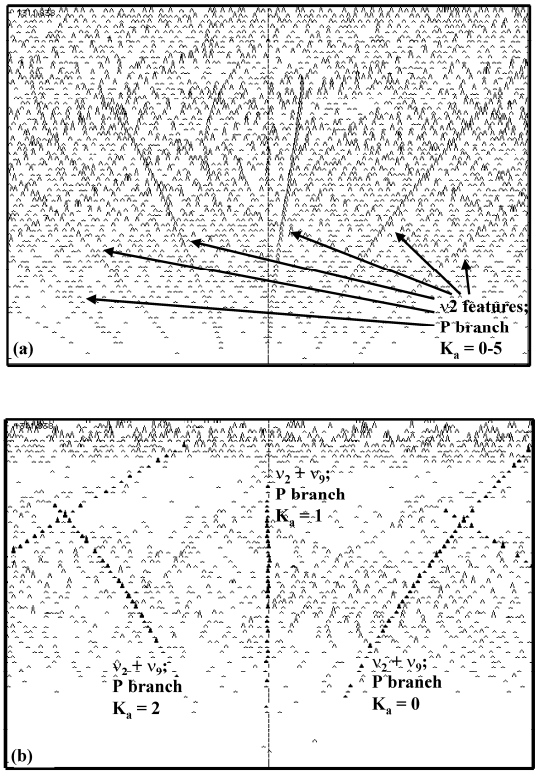
ν2 features;
P branch
Ka = 0-5
(a)
ν2 + ν9;
P branch
Ka = 1
ν2 + ν9;
P branch
Ka = 2
ν2 + ν9;
P branch
Ka = 0
(b)

Figure 5

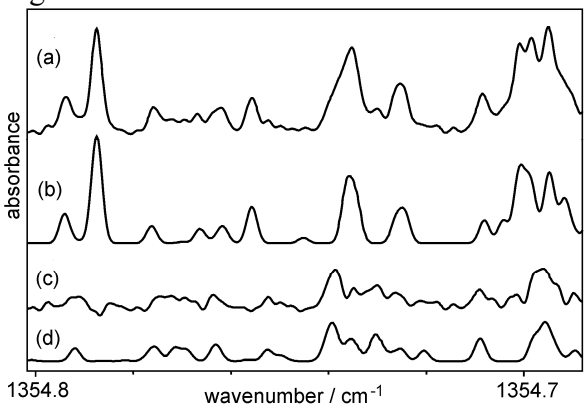

Figure 6.

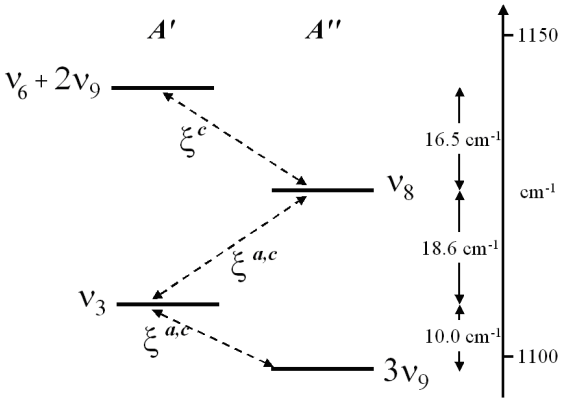

Fig 7

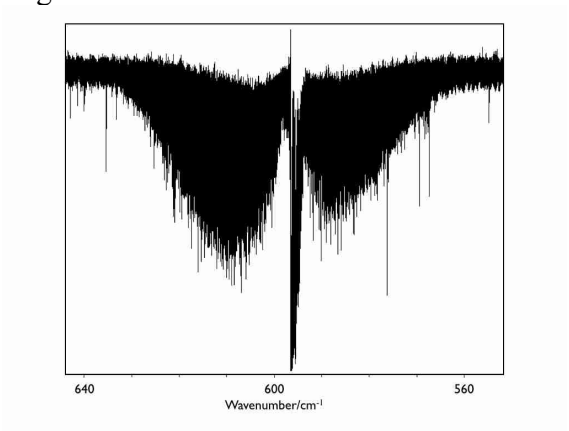
640
600
560
Wavenumber/cm-1

Fig 8

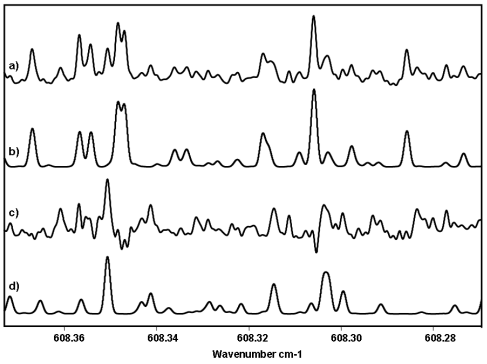
a)
b)
c)
d)
608.36
608.34
608.32
608.30
608.28
Wavenumber cm-1